

High Heat Resistant Coatings by Means of Gas Tunnel Type Plasma Spraying

IEPC-2011-017

*Presented at the 32nd International Electric Propulsion Conference,
Wiesbaden • Germany
September 11 – 15, 2011*

Akira Kobayashi¹
Osaka University, Ibaraki, Osaka 567-0047, Japan

Yasutaka Ando²
Ashikaga Institute of Technology, Ashikaga, Tochigi 326-8558, Japan

and

Kazuya Kurokawa³
Hokkaido University, Sapporo, Hokkaido 060-8628, Japan

Abstract: Zirconia sprayed coatings are widely used as thermal barrier coatings (TBC) for high temperature protection of metallic structures in gas turbine hot section components such as burners, transition ducts, vanes and blades. However, their use in diesel engine combustion chamber components has the long run durability problems, such as the spallation at the interface between the coating and substrate due to the interface oxidation. Although zirconia coatings have been used in many applications, the interface spallation problem is still waiting to be solved under the critical conditions such as high temperature and high corrosion environment. In this study, ZrO₂ (YSZ) composite coatings (TBCs) with Al₂O₃ and La₂Zr₂O₇ were deposited on SS304 substrates by gas tunnel type plasma spraying. The performance such as the structural, mechanical properties and electrochemical corrosion behaviors was investigated and the results are discussed based on the thickness and the microstructure of the coatings.

I. Introduction

Zirconia sprayed coatings are widely used as thermal barrier coatings (TBC) for high temperature protection of metallic structures in gas turbine hot section components such as burners, transition ducts, vanes and blades. However, their use in diesel engine combustion chamber components has the long run durability problems, such as the spallation at the interface between the coating and substrate due to the interface oxidation [1]. Although zirconia coatings have been used in many applications, the interface spallation problem is still waiting to be solved under the critical conditions such as high temperature and high corrosion environment [2,3]. Generally the TBCs have to encounter low-quality fuels during operation, the impurities in these highly contaminated fuels combine to form molten salts, such as sodium sulfate and vanadium compounds and deposit on the coating surface in the combustion environment, thus giving rise to hot corrosion problems. Hence, it should be noted that the hot corrosion resistance mechanism of the TBC material against different kinds of corrosive environments is also one of the imperative factors that must be taken into account along with other factors such as thermal conductivity, phase stability, thermal

¹Associate Professor, JWRI, kobayasi@jwri.osaka-u.ac.jp.

² Professor, Faculty of Engineering, yando@ashitech.ac.jp

³ Professor, Graduated School of Engineering, kurokawa@eng.hokudai.ac.jp.

expansion coefficient and mechanical properties of the TBC material while exploring for new TBC materials or while validating the existing one as a promising TBC material.

The gas tunnel type plasma spraying developed by the author can make high quality ceramic coatings such as Al_2O_3 and ZrO_2 coating compared to other plasma spraying methods [4,5]. A high hardness ceramic coating such as Al_2O_3 coating by the gas tunnel type plasma spraying, were investigated in the previous study [6,7]. The Vickers hardness of the zirconia (ZrO_2) coating increased with decreasing spraying distance, and a higher Vickers hardness of about $Hv=1200$ could be obtained at a shorter spraying distance of $L=30$ mm. ZrO_2 coating formed has a high hardness layer at the surface side, which shows the graded functionality of hardness [8,9,10].

In this study, ZrO_2 composite coatings (TBCs) with Al_2O_3 and $\text{La}_2\text{Zr}_2\text{O}_7$ were deposited on SS304 substrates by gas tunnel type plasma spraying under optimum spraying conditions. The performance such as the structural, mechanical properties and electrochemical corrosion behaviors was investigated and the results are discussed based on the thickness and the microstructure of the coatings.

II. Experimentals

The gas tunnel type plasma spraying torch used is shown in Fig.1. The experimental method to produce the ceramic coatings by means of the gas tunnel type plasma spraying is as follows. After igniting plasma gun, the main vortex plasma jet is produced in the low pressure gas tunnel. The spraying powder is fed from center inlet of plasma gun. The coating was formed on the substrate traversed at the spraying distance of 50mm. The experimental parameters for the plasma spraying were selected based on previous reports [4-7]. The power input to the plasma torch was about $P=25$ kW, and the power input to the pilot plasma torch, which was supplied by the power supply PS-1, was turned off after starting of the gas tunnel type plasma jet.

For this purpose, 8 wt% Y_2O_3 stabilized ZrO_2 (8YSZ), alumina (Al_2O_3) and lanthanum zirconate ($\text{La}_2\text{Zr}_2\text{O}_7$) powders were commercially procured with average size ranging from 10-60 μm . 7 slpm of argon gas was used as the carrier gas to carry the powder from the feeder at the rate of 15-20 grams per minute to form a coating on SS304 substrate under a total (primary and vortex) argon gas flow rate of 180 slpm.

Regarding the analysis of coating properties, the microstructure of the cross section of ZrO_2 composite coating was observed by an optical microscope in this research. The microscope is equipped with a CCD camera for image acquisition. Micrographs with two magnifications (200 X and 400 X) taken on polished cross sections are used for determining the total porosity and coating thickness by using image analysis software. The microstructure of the cross section of ZrO_2 composite coating was observed by an optical microscope. The Vickers hardness Hv_{50} , Hv_{100} of the sprayed coatings was measured at the non-pore region in those cross sections under the condition that the load weight was 50g, 100 g and its load time was 15s, 25 s. The Vickers hardness: Hv_{100} was calculated as a mean value of 10 point measurements. The distribution of the Vickers hardness in the cross section of the coating was measured at a fixed distance from the coating surface in the thickness direction.

The electrochemical measurements were carried out on the samples with open circuit potential (OCP)–time measurements, potentiodynamic polarization, and electrochemical impedance spectroscopic studies, using a conventional three-electrode cell connected with a potentiostat (Autolab PGSTAT galvanostat/potentiostat). The test electrolytes for electrochemical investigations were 0.1 mol of Na_2SO_4 . A saturated calomel reference electrode (SCE) and a platinum counter electrode were employed. The sample surface was cleaned by distilled water. The exposed surface area of all specimens was fixed at 1 cm^2 and the remaining portion except for the exposed area was painted with a strong adhesive silicon bond in order to prevent the initiation of crevice corrosion. In order to establish the open circuit potential (OCP), prior to the polarization measurements, the samples were immersed in the solution for about 60 min. The applied alternating potential had root mean square amplitude of 10 mV on the OCP. After getting the stable OCP, the upper and lower potential limits of linear sweep voltammetry were set at +200 and

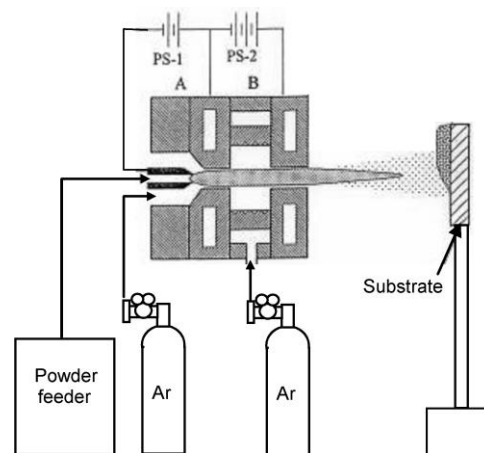


Figure 1. Schematic of the gas tunnel type plasma spraying torch.

-200 mV respectively with reference to OCP. The sweep rate was 1 mVs^{-1} . The corrosion potential E_{corr} , corrosion current I_{corr} and corrosion rate were determined by the Tafel extrapolation method.

III. Result and Discussion

3.1 YSZ+Al₂O₃ composite coating

Typical optical cross sectional micrographs for thermal barrier coatings are shown in Fig.2. Those are the ZrO₂ composite coatings of 20% and 50% Al₂O₃ mixture, respectively. The coatings are porous and one of lamellar structure which is typical characteristic for as-sprayed coatings. The thickness was about 150 μm. The composition of the microstructure is represented by gray level variation. It consisted of 2 different layers, white and gray layers were deposited alternatively. The analysis by EPMA revealed that white was zirconia (ZrO₂) and gray was alumina (Al₂O₃). Pores appear to be dark, which permit them to be distinguished and quantified by image analysis. The hardness distribution of the ZrO₂ composite coating has remarkable graded functionality in the case of large Al₂O₃ mixing ratio. Because, the part near the substrate did not change so much, but the Vickers hardness near the coating surface became much higher. Fig.3 shows the distribution of Vickers hardness: Hv_{50} of the zirconia/alumina composite coating shown in Fig.2 (coating thickness: about 150 μm). The distribution of this composite coating has a highest value in the coating at the surface side: The maximum hardness was near to $Hv_{50} = 1300$ at the the coating surface of $l=40 \mu\text{m}$, and decreased linearly like towards the substrate side. While, the porosity profile over the coating cross-section (Fig.4) gives an almost linearly graded distribution, increasing from the surface of the coatings towards the surface of the substrate. In as- sprayed condition the porosity variation ranges from 18.95% to 33.23% from the surface of the coatings to the surface of the substrate. Although lower porosity can increase the average hardness of the coatings, alumina present in the coatings is the origin of the improved hardness because higher mixing ratio of alumina results in lower porosity.

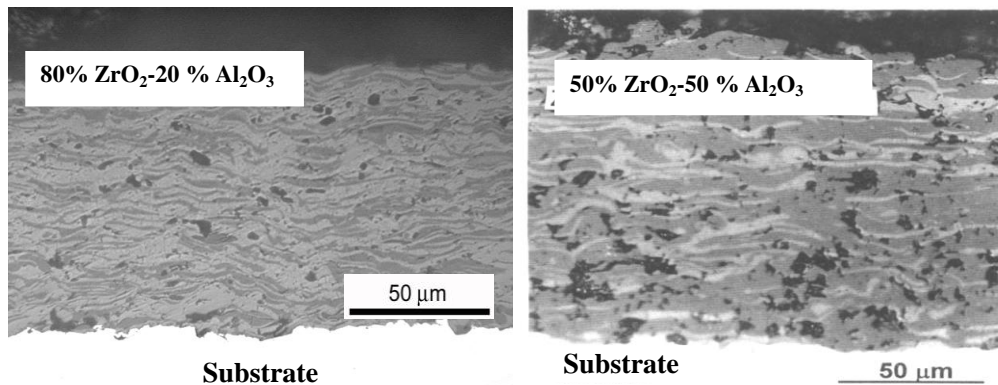


Figure 2. Micrographs of the cross-section of coating samples.

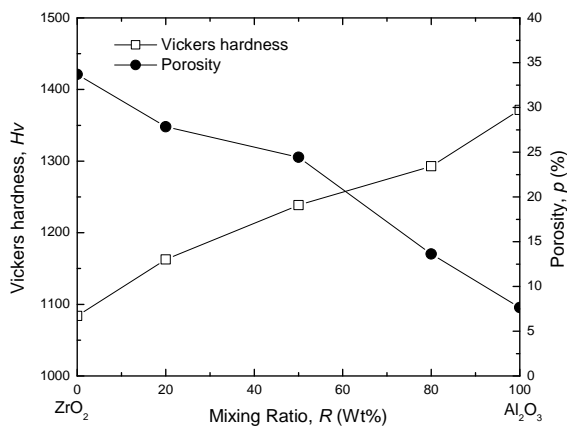


Figure 3. Vickers hardness and porosity of ZrO₂/Al₂O₃ composite coatings.

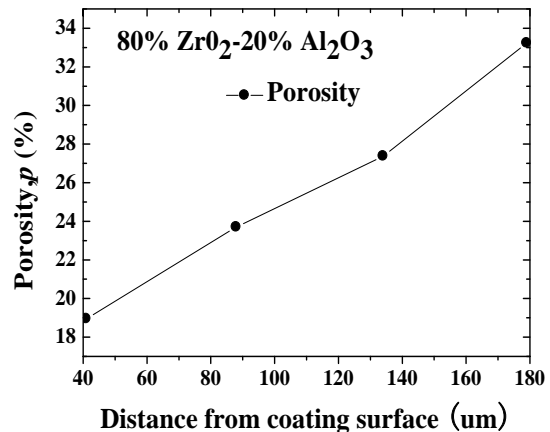


Figure 4. Porosity distributions over the coating cross-section.

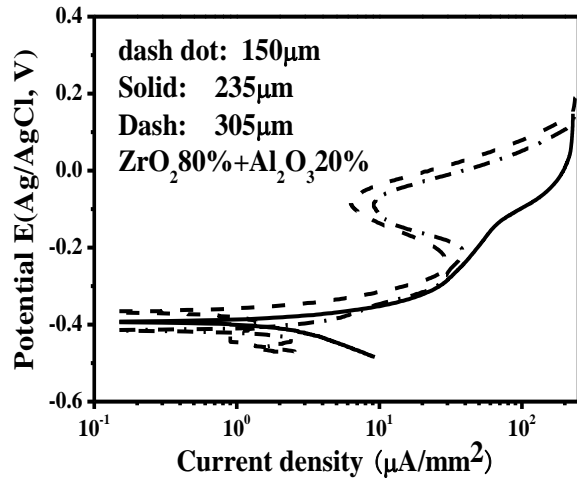


Figure 5. Corrosion curves of ZrO_2 composite coatings.

So, in conclusion, higher thickness and lower porosity sprayed coatings lead to increase of corrosion resistance because both higher thickness and lower porosity provide stronger diffusion resistance to prevent the anodic oxidants of the corrosion solution from accessing the interface of the coated samples.

3.2 YSZ+ $La_2Zr_2O_7$ composite coating

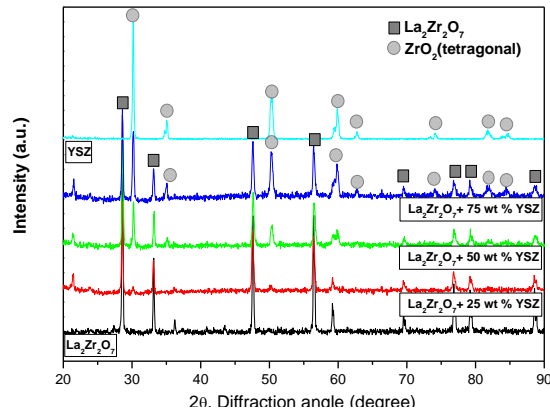


Figure 6. XRD pattern of YSZ+ $La_2Zr_2O_7$ composite coatings.

Fig.6 shows the XRD patterns of plasma sprayed ZrO_2 (YSZ)+ $La_2Zr_2O_7$ composite coatings. The XRD pattern revealed that the pyrochlore phase of $La_2Zr_2O_7$ and tetragonal phase of ZrO_2 were stable even in the coatings obtained at higher plasma power under the optimized plasma torch spraying conditions. The main feature of this XRD investigation is that the obtained peaks belonging to the pyrochlore structure shift slightly towards smaller 2θ value and cause larger lattice parameter than that of the initial powder. Furthermore, the stoichiometric ratios of ZrO_2/La_2O_3 varied significantly in the coating compared to the ratio in the initial powder. The same trend is further continued in composite coating also. This deviation can be attributed to the loss of La_2O_3 in $La_2Zr_2O_7$ during in-flight at high temperature zone. However, the above variation does not affect the pyrochlore structure because of the considerable solubility range of $La_2Zr_2O_7$ from 53.6 wt% La_2O_3 and 46.4 wt% ZrO_2 to 60.4 wt% La_2O_3 and 39.6 wt% ZrO_2 whereby the crystalline structure and properties remain unaffected [11].

In general, ZrO_2 is thermally more stable than La_2O_3 in pyrochlore structure; hence the subsequent different evaporation rates of the components might lead to the stoichiometric change while spraying in high temperature

Regarding the anodic corrosion polarization characteristics of ZrO_2 composite coating, Fig.5 presents the anodic corrosion polarization characteristics of the samples coated with different thickness of 80% ZrO_2 + 20% Al_2O_3 mixture coating. All the curves are obtained from their first polarization scan. From the curves, it is clear that their corrosion potentials increase with the coating thickness. However, their corrosion current shows a complicated tendency with the coating thickness, which is possibly due to the complex bonding states of the coatings to the substrates because the effective area of the substrate exposed to the corrosion media is responsible for the corrosion current. The corrosion potential goes up slightly with the coating thickness. Theoretically, high corrosion potential means lower electrochemical activity and higher oxidation resistance.

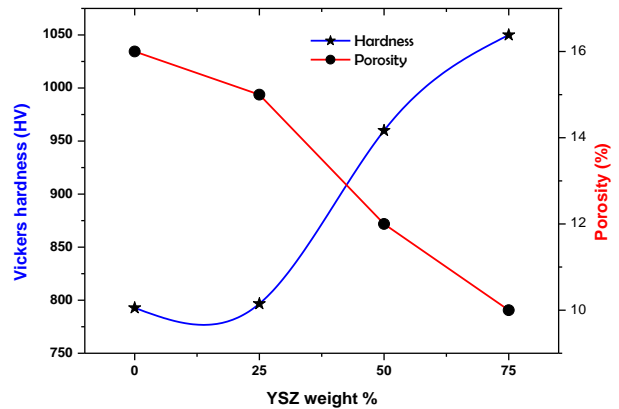


Figure 7. Vickers hardness and porosity of YSZ+ $La_2Zr_2O_7$ composite coatings.

plasma jet. Meanwhile, tetragonal phase zirconia did not deviate from its initial stoichiometric even though its melting fraction is high. Furthermore, the observation of the patterns shows that the tetragonal phase gradually increased with respect to weight percentage of YSZ without disturbing the pyrochlore structure.

The typical microstructure of the gas tunnel type plasma sprayed $ZrO_2+La_2Zr_2O_7$ composite coating is porous and of lamellar structure like the $ZrO_2+Al_2O_3$ composite coating which is a unique characteristic of this kind of spraying, but it could be controlled by optimizing the spraying conditions. Herein, the splats are separated by interlamellar pores resulting from rapid solidification of the lamellae. Sporadically, fine voids also appear nearby the un-melted particles along with few cracks due to thermal stresses and tensile quenching relaxation stresses. Favorably, the presence of cracks also increases the strain tolerance and enhances the thermal shock resistance of TBCs in service. Moreover, the porosity of $ZrO_2+La_2Zr_2O_7$ composite coating microstructure significantly varied with respect to the presence of YSZ content. Fig. 7 shows the porosity and Vickers hardness of the composite coatings as a function of YSZ weight percentage at steady state plasma spraying condition. YSZ coatings show least porosity (10%) and $La_2Zr_2O_7$ coatings reveal maximum porosity (16%) while in its composite coating the porosity gradually decreases while increasing the YSZ content in the coating.

This is mainly caused due to the variation in the melting fraction of the in-flight ZrO_2 and $La_2Zr_2O_7$ particles in the high temperature plasma jet. In plasma sprayed coatings the porosity and microhardness are inversely proportional to each other which has already been proven by many researchers. The same trend was revealed in the $ZrO_2+Al_2O_3$ composite coating. Due to the same reasons herein the Vickers hardness of the composite coating varied with respect to the porosity. The Vickers hardness of the $La_2Zr_2O_7$ composite coating is relatively lower than YSZ coating i.e 780 Hv. In the meantime, the hardness increases on increasing the YSZ content in the composite coating.

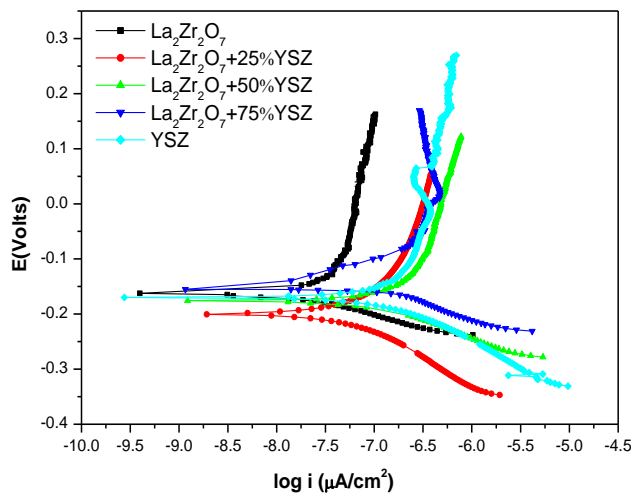


Figure 8. Potentiodynamic polarization curves of YSZ + $La_2Zr_2O_7$ composite coatings

Furthermore, theoretically the corrosion rate is directly proportional to the corrosion potential. Hence here the composite coatings i.e $La_2Zr_2O_7 + 25\%$ YSZ has the lowest current density and also the corrosion rate is found to be minimum compared to all other coatings as shown in Table 1. The above results confirm that apart from the coating microstructure the corrosion kinetics also play a vital role in determining the electrochemical corrosion behavior of the coatings.

Typical potentiodynamic polarization curves of the $ZrO_2+La_2Zr_2O_7$ composite coatings and its corresponding values are respectively shown in Fig. 8 and Table 1. This electrochemical impedance spectroscopy is a powerful technique to study the electrochemical properties of the plasma sprayed coatings due to its high sensitivity to the coating microstructure. The observation from this result reveals that pure YSZ and $La_2Zr_2O_7$ coatings have poor corrosion potential, but their composite coatings seem to be good. In particular, the polarization curve for 25% YSZ+ $La_2Zr_2O_7$ coating had a significantly higher corrosion potential (-0.133 V) than that of other composite coatings. The results confirmed that 25% YSZ+ $La_2Zr_2O_7$ coatings exhibited a superior electrochemical behavior than pure and other composite coatings by virtue of more noble corrosion potential, although all the curves were characterized by a very similar trend.

Table 1 Corrosion results of YSZ+ $La_2Zr_2O_7$ composite coatings.

| Coatings | E_{corr} V | bc V/dec | ba V/dec | $I_{corr} \times 10^{-8}$ Acm^{-2} | Corrosion Rate, mm/y 10^{-4} |
|------------------------|-----------------|-------------|-------------|---|--|
| $La_2Zr_2O_7$ | -0.186 | 0.016 | 0.001 | 1.409 | 5.282 |
| 25% YSZ+ $La_2Zr_2O_7$ | -0.133 | 0.007 | 0.017 | 0.334 | 1.250 |
| 50% YSZ+ $La_2Zr_2O_7$ | -0.200 | 0.015 | 0.015 | 0.609 | 2.283 |
| 75% YSZ+ $La_2Zr_2O_7$ | -0.176 | 0.005 | 0.017 | 1.067 | 4.002 |
| YSZ | -0.169 | 0.056 | 0.027 | 3.804 | 14.26 |

IV. Conclusion

The high energy density and high efficiency gas tunnel type plasma spray torch was employed to prepare different kinds of $ZrO_2 + Al_2O_3$ and $ZrO_2 + La_2Zr_2O_7$ composite coatings on SS304 substrates under optimized spraying conditions for TBC application. The structural, mechanical and electrochemical corrosion properties of the coatings were examined and the following conclusions are made:

- (1) With an increase in the mixing ratio of Al_2O_3 , the Vickers hardness of the ZrO_2 coating increases while its porosity decreases. In the microstructure of $ZrO_2 + Al_2O_3$ composite coating the porosity was minimum near the surface and maximum near the substrate.
- (2) Thicker coatings and higher content of Al_2O_3 , give higher corrosion potential due to lower oxidation reaction rate on the interface. Low porosity is the key factor for improving the corrosion resistance of the coatings.
- (3) While spraying at high plasma power $La_2Zr_2O_7$ coating deviates from its stoichiometric due to the loss of La_2O_3 . With an increase in the mixing ratio of ZrO_2 , the Vickers hardness of the $La_2Zr_2O_7$ coating increases.
- (4) Electrochemical corrosion behavior of $ZrO_2 + La_2Zr_2O_7$ composite coating seems to be good compared to its individual coatings. Apart from the coating microstructure the corrosion kinetics also plays a vital role in determining the electrochemical corrosion behavior of $ZrO_2 + La_2Zr_2O_7$ composite coatings.

References

- ¹R. Vassen, G. Kerckhoff, and D. Stoeber, "Development of a Micromechanical Life Prediction Model for Plasma Sprayed Thermal Barrier Coatings," *Mater. Sci. Eng.*, A303, 2001, pp. 100-109.
- ²P. Ramaswamy, S. Seetharamu, K.B.R.Varma, and K.J. Rao, "Thermal Shock Characteristics of Plasma Sprayed Mullite Coatings," *J. Therm. Spray Technol.* Vol.7(4), 1999, pp. 497-505.
- ³Zhenhua Xu, Xinghua Zhong, Jiangfeng Zhang, Yanfei Zhang, Xueqiang Cao, Limin He, "Effects of Deposition Conditions on Composition and Thermal Cycling Life of Lanthanum Zirconate Coatings," *Surf. Coat. Tech.* Vol.202, 2008, pp. 4714-4720.
- ⁴Y.Arata, A. Kobayashi, and Y. Habara, "Ceramic Coatings Produced by means of a Gas Tunnel - Type Plasma Jet," *J. Applied Physics*, 62, 1987, pp.4884-4889.
- ⁵Y.Arata, A. Kobayashi and Y. Habara, "Formation of Alumina Coatings by Gas Tunnel Type Plasma Spraying (in Japanese)," *J. High Temp. Soc.*, Vol.13, 1987, pp.116-124.
- ⁶A.Kobayashi, S. Kurihara, Y. Habara, and Y. Arata, "Relation between Deposit Characteristics and Ceramic Coating Quality in Gas Tunnel Type Plasma Spraying," *J. Weld. Soc. Jpn.*, Vol.8, 1990, pp.457-463.
- ⁷A.Kobayashi, "Property of an Alumina Coating Sprayed with a Gas Tunnel Plasma Spraying," *Proc. of ITSC*, 1992, pp.57-62.
- ⁸A.Kobayashi, "Formation of High Hardness Zirconia Coatings by Gas Tunnel Type Plasma Spraying," *Surface and Coating Technology*, Vol.90, 1990, pp.197-202.
- ⁹A.Kobayashi and T. Kitamura, "High Hardness Zirconia Coating by Means of Gas Tunnel Type Plasma Spraying(in Japanese)," *J. of IAPS*, Vol.5, 1997, pp.62-68.
- ¹⁰A.Kobayashi, T. Kitamura, "Effect of Heat Treatment on High-Hardness Zirconia Coatings Formed by Gas Tunnel Type Plasma Spraying," *VACUUM*, Vol.59-1, 2000, pp.194-202.
- ¹¹S. Yugeswaran, Akira Kobayashi, P.V. Ananthapadmanabhan, L. Lusvarghi, "Influence of processing variables on the formation of $La_2Zr_2O_7$ in transferred arc plasma torch processing" *Current Applied Physics*, In Press.